Semiconductor physics

Processes of mass transfer and formation of inversion and graded-gap layers in CdTe-based solid solutions irradiated with nanosecond pulses

S.M. Levytskyi

V. Lashkaryov Institute of Semiconductor Physics, NAS of Ukraine, Kyiv, Ukraine
E-mail: levytskyism@gmail.com

Abstract. This article presents the results of the study of modification of CdTe surface layer using optical methods as well as a direct effect of laser irradiation on the properties of CdTe using the induced dynamic lattice method. The effectiveness of optical probing in the study of laser-induced processes in A_2B_6 compounds has been demonstrated. In addition to optical methods, the induced dynamic lattice method has been used to determine the properties of the studied material before and after laser irradiation. The photoluminescence of laser-modified CdTe samples has been also studied. The obtained results significantly expand current understanding of the interaction mechanisms between high-power laser radiation and semiconductor structures. This opens up promising opportunities for precise control over the physical characteristics of materials during the development of new electronic devices.

Keywords: A^2B^6, CdTe, laser irradiation, photoluminescence, laser doping.

https://doi.org/10.15407/spqeo29.03.317
PACS 61.46.Df, 61.72.uf

Manuscript received 16.02.26; revised version received 26.08.26; accepted for publication 16.09.26; published online 25.09.26.

1. Introduction

A^2B^6 semiconductors, particularly cadmium telluride (CdTe), are key materials in modern optoelectronics, photonics, and nuclear detection due to their unique optical, electrical, and structural properties [1–4]. CdTe has a direct band gap of approximately 1.44 eV at room temperature, high carrier mobility, and the ability to efficiently absorb radiation in the visible and near-infrared ranges. These characteristics make it indispensable for creating solar cells, X-ray and gamma-ray detectors, and infrared sensors. However, optimizing the properties of CdTe often requires modification of surface layers, including doping and formation of inversion or variable-gap structures, which improves the efficiency of devices and expands their functionality.

In recent decades, laser technology has become a powerful tool for precision semiconductor processing. Nanosecond laser pulses provide localized heating, melting, and mass transfer without significant substrate damage, which is especially important for brittle materials like CdTe. These processes induce phase transitions, impurity diffusion, and defect restructuring, leading to formation of layers with controlled properties. For example, laser doping allows creating *p-n* junctions or heterostructures of high performance, which are critical for manufacturing diode detectors and photo-detectors. However, the mechanisms of these processes are complex due to nonlinear effects such as temperature gradients, interference phenomena, and defect generation, requiring detailed study.

Optical diagnostic methods play a central role in the study of laser-induced surface modification. Optical probing, based on reflectivity dynamics analysis, allows for real-time monitoring of phase transitions, despite the absence of a sharp reflection jump upon melting of A^2B^6, unlike A^4 or A^3B^5 semiconductors. Moreover, induced dynamic grating (IDG) technique provides information on heat and mass transfer by measuring diffusion coeffi-cients and thermal diffusivity. Photoluminescence (PL) serves as a sensitive indicator of defects and recombina-tion processes, revealing influence of laser irradiation on the electronic structure. Despite the progress, many aspects of laser modification of CdTe remain poorly understood. In particular, clarification of the mass transfer kinetics, the role of interference in reflection, and formation of long-term electronic states are required. Previous studies [1–15] demonstrate the efficiency of laser doping for CdTe and CdZnTe, but the focus on combined use of optical methods with IDG and PL is limited. This work focuses on a comprehensive study of laser-induced processes in CdTe using nanosecond pulses of a ruby laser. We analyze the reflection dynamics to determine melting modes, measure the thermal diffu-sivity by using NDR before and after irradiation, and study PL to evaluate the defect structure. The obtained results can be used to optimize laser technologies for fabrication of high-performance CdTe-based devices.

The aim of the study is to establish correlations between laser irradiation parameters, phase transition kinetics, and optoelectronic properties of modified layers to provide better understanding of laser-induced processes in CdTe.

2. Optical methods for studying processes of modification of CdTe surface layers

2.1. Features of optical probing method applied to A^2B^6 semiconductors

Optical probing [10–14] exploits the fact that most semiconductors, particularly A^4(Si, Ge) and A^3B^5 (GaAs, InSb, GaSb), upon melting, pass to a metallic state characterized by high values of the reflection coefficient. Presence of a region of increased reflectivity in oscillograms of the reflected probing radiation indicates a 'solid–melt' phase transition. The lifetime of the phase with the increased reflectivity corresponds to the duration of the existence of the liquid phase. Fig. 1 shows typical oscillograms of reflected probing radiation under laser irradiation by using Si as an example. The duration of the existence of the liquid phase is denoted as τ. The conditions of the laser irradiation are indicated in the caption to the figure.

A different situation is observed for A^2B^6 semiconductors, namely melting of A^2B^6 does not lead to a semiconductor-metal phase transition and no significant change in the reflection coefficient takes place. Therefore, the question arises about the possibility of using the optical probing method to study the kinetics of laser-induced phase transformations in these semiconductors.

Previous studies with optical diagnostics of processes in CdTe [1–10] and CdMnTe compound [11] have shown that this method allows one to study the kinetics of laser-induced phase transformations in these semiconductors as well. Details of the method for studying the dynamics of reflection at the wavelengths $\lambda_1 = 1.06$ μm and $\lambda_2 = 0.53$ μm are described in [14]. The changes in the reflection coefficient in the oscillograms of the reflected radiation in this situation are associated with the temperature dependence of the reflection coefficient and interference phenomena in the melt–solid structure.

In this study, additional measurements of the reflectivity of CdTe were carried out at the same wavelengths over a wide range of irradiation energy densities. The measurement results completely agree with the data obtained in [13, 14], confirming the measurements reliability.

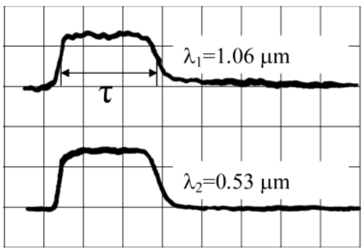

Fig. 1. Dynamics of reflectivity $R(t)$ of Si at two wavelengths under irradiation with a ruby laser pulse with $W = 0.23$ J/cm^2 and pulse duration of 80 ns (horizontal division value is 100 ns).

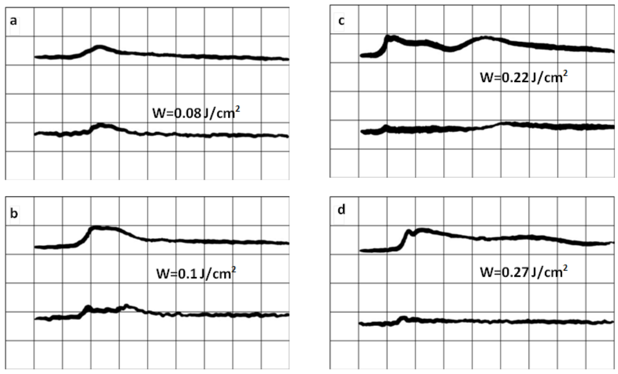

Fig. 2. Dynamics of the reflectivity of CdTe samples under laser irradiation with different energy densities. The upper scan lines correspond to $\lambda_1 = 1.06$ μm, the lower ones to $\lambda_2 = 0.53$ μm (the horizontal division value is 100 ns).

CdTe samples were irradiated with ruby laser pulses in the energy density range from 0.08 to 0.32 J/cm^2. The laser optical design ensured high homogeneity within the laser spot due to the extremely broad spectral composition of the generated irradiation with the energy of 1.5 J. The inhomogeneity of the single-pulse energy distribution within the spot did not exceed ±5%. The irradiation energy was reproduced from pulse to pulse with a deviation of no more than ±1.5%. The pulse duration was 80 ns.

Fig. 2 shows how reflectivity dynamics changes at increasing the irradiation energy density. The reflected signal oscillograms show changes in the reflectivity for both probing irradiation wavelengths, these changes being more pronounced for λ_1.

The edge of the fundamental radiation absorption band of single-crystalline CdTe is known to correspond to the wavelength $\lambda = 0.832$ μm, *i.e.*, probing irradiation with λ_1 is almost not absorbed in the material at $T = T_0 = 300$ K, while irradiation with λ_2 is almost completely absorbed by a 10^{-5} cm thick layer [15].

Three different modes of laser irradiation of CdTe can be distinguished for irradiation energy densities E below the threshold of material destruction. At $E \approx 0.08$ J/cm^2, an increase in the reflectivity R is observed at both wavelengths of the probing radiation (Fig. 2a), which can be explained by the temperature dependence of the optical parameters of solid CdTe. At $E = 0.1$ J/cm^2, differences in the time dependences of the reflection coefficient are visible (Fig. 2b).

At λ_1, further increase in R is observed. At λ_2, two weak maxima appear apparently indicating beginning of melting. The first maximum of the reflectance of the probing radiation at λ_2 is reached at the beginning of melting, at the moment of the greatest heating of the surface. The subsequent decrease and then increase in R up to the second maximum is related to interference of the radiation during reflection from the sample surface and the moving phase boundary. An intermediate minimum at λ_1 at the beginning of the melting is not observed due to a more complex temperature dependence of the optical absorption at λ_1, the magnitude of which is affected by an increase in absorption upon heating on the one hand, and by a temperature-induced narrowing of the band gap on the other hand.

After increasing E to 0.17 J/cm^2, the nature of the change in R is the same for both wavelengths, with the distance between the maxima being greater for λ_2. Further increase in the energy density from this value up to 0.22 J/cm^2 leads to an increase in the time interval between these maxima and does not change the nature of the dependence $R(t)$ at λ_2. However, a more complex dependence $R(t)$ is observed at λ_1, which is explained by the temperature dependence and interference effects on the resulting multilayer system (Fig. 2c).

Further increase in the irradiation energy density to 0.27 J/cm^2 results in blurring of the maxima, particularly the second maximum, complicating diagnostics (Fig. 3d). For all the studied modes (except for W = 0.27 J/cm^2), the initial and final values of the reflection coefficient are identical, indicating absence of damage or other significant surface changes.

As a result of the experiments, laser-modified samples were prepared for study by the induced dynamic grating method.

2.2. Induced dynamic grating method

The dynamic grating method was used to study thermal diffusivity of CdTe samples before and after laser irradiation. This method is based on creation of a non-stationary thermal grating in the sample by using interfering laser beams [16], thereby creating an initial distribution of heat sources with a specified periodic structure. A method of diffraction probing with a continuous laser (CW laser diffraction probing) is used to read the grating. The temperature conductivity of the material can be determined from the measured diffraction relaxation time.

The measurements were carried out with a developed laser measuring system. CdZnTe samples with the zinc content of no more than 4% were used as test objects. To determine the effect of laser irradiation, unirradiated samples and a sample irradiated with a ruby laser pulse of 80 ns duration with an energy density of 0.32 J/cm^2 were used. According to optical-pyrometric measurements under this irradiation mode, the liquid phase lifetime reaches 1.6 µs, and the maximum surface brightness temperatures exceed 2000 K (Fig. 3).

The studies were performed in reflected light. Thermal gratings with the periods of 25 and 50 µm were excited at the wavelength of 532 nm, and the pump pulse duration was 60 ps. The pump energy density in the sample plane was 0.9 mJ/cm^2. Probing was performed at the wavelength of 633 nm. The time dependence of the diffraction signal intensity was approximated by an additional error function $S = S_0 A \cdot erfc\left(\sqrt{\frac{t}{\tau}}\right)$, where S_0, A, and τ are the fitting coefficients, and t is the time, respectively.

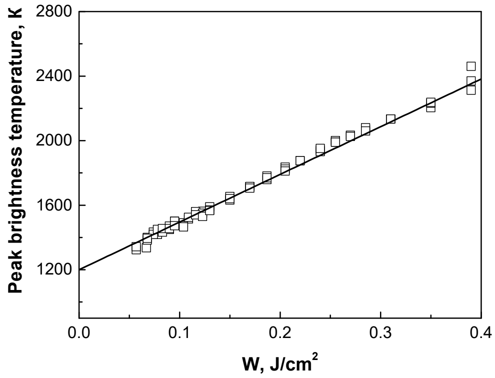

Fig. 3. Peak brightness temperature of the laser heated zone of CdTe *versus* irradiation energy density.

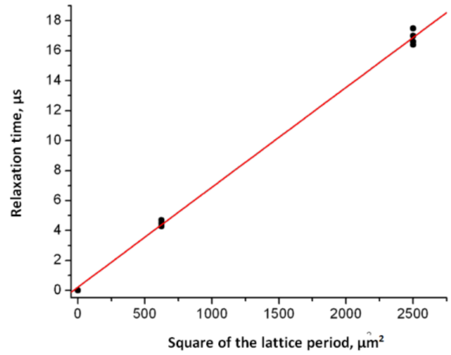

Fig. 4. Lifetime of the thermal grating in the CdZnTe crystal versus square of the grating period.

The thermal grating relaxation time τ_D increases with the grating period Λ and is linearly dependent on the square of the period (Fig. 4). Moreover, no significant differences between the initial and laser-modified samples were observed. The thermal grating diffraction efficiency was ~$5\cdot10^{-6}$.

Temperature conductivity can be found from the thermal grating relaxation time using the following expression:

$$a = \frac{\Lambda^2}{4\pi\tau_D}. \quad (1)$$

The value of the temperature conductivity calculated based on the relaxation time was $(3.67 \pm 0.17)\cdot10^{-2}$ cm^2/s, which agrees well with the known thermophysical parameters values (Table 1).

An acoustic signal was also clearly observed in the experiments. In the Fourier spectrum, the frequencies of 7.6 and 29.6 MHz correspond to acoustic vibrations in air (380 m/s) and in the crystal (1480 m/s), respectively. Other frequencies are associated with interference. No differences in the acoustic signals for the initial and laser-modified samples were detected.

The results shown in Fig. 5 indicate the formation of a long-range electron lattice upon excitation of the laser-modified sample.

Table 1. Thermophysical and optical properties of CdTe [10-13].

Parameter		Solid	Liquid
Density	g/cm^3	$(5.887…1.165)\cdot10^{-4}T$	$(6.158…3.622)\cdot10^{-4}T$
Thermal conductivity	W/(cm·K)	$15.07/T$	$2\cdot10^{-15}\cdot T\cdot[(2.213…3.654)\cdot10^{-3}\cdot T + 1.52\cdot10^{-6}\cdot T^2)]$
Heat capacity	J/(g·K)	$0.21 + 9.7\cdot10^{-5}\cdot T$	0.314
Temperature conductivity	cm^2/s	0.036 (T = 300 K) 0.006 (T = 1300 K)	0.0008 (T = 1365 K)
Melting point	K	1365	
Boiling point	K	No data	
Heat of fusion	J/g	331	
$n(\lambda = 694$ nm$)$		3.04	3.04
$\alpha(\lambda = 694$ nm$)$	Sm^{-1}	$83.96\cdot T + 3.54\cdot10^4$	$1.5\cdot10^5$
$n(\lambda = 532$ nm$)$		3.32	
$\alpha(\lambda = 532$ nm$)$	Sm^{-1}	$6.7\cdot10^4$	
$n(\lambda = 633$ nm$)$		2.6	
$\alpha(\lambda = 633$ nm$)$	Sm^{-1}	$3.694\cdot10^4$	

Comparing the diffraction signals from the initial and laser-modified samples, one observes a pronounced thermal kinetics (τ ~ 1…10 µs depending on the grating period) and a fast component (τ ~ 10 ns for any period) due to the amplitude grating in the first case.

When a laser-modified sample is excited, the signal exhibits a fast component of amplitude grating (τ ~ 10 ns) and a long-term kinetics (τ ~ 10 ms regardless of the grating period), presumably electronic one (Fig. 6).

The observed kinetics are possibly related to excitation of defects formed after irradiation. Moreover, most of the pump energy is apparently spent to excite the long-term grating. A thermal grating with the period of 50 µm was also detected in the experiment.

Study of the laser-modified CdZnTe sample over a period of 25 µm showed formation of a short-term grating in addition to the phase grating. Apparently, the short-term grating has an amplitude nature (grating of the reflection coefficient) since it is phase-shifted relative to the thermal grating by π/2 (Fig. 7). According to various measurements, the characteristic lifetime of the short-term grating was 20…40 ns regardless of the period. More precise measurements of the relaxation time of this component are difficult due to its small amplitude and a need to carefully select the phase difference between the scattering background and the diffraction signal.

The existence of the fast amplitude component is most likely due to thermal reflection and heat transfer from the surface into the sample *via* vertical heat transfer.

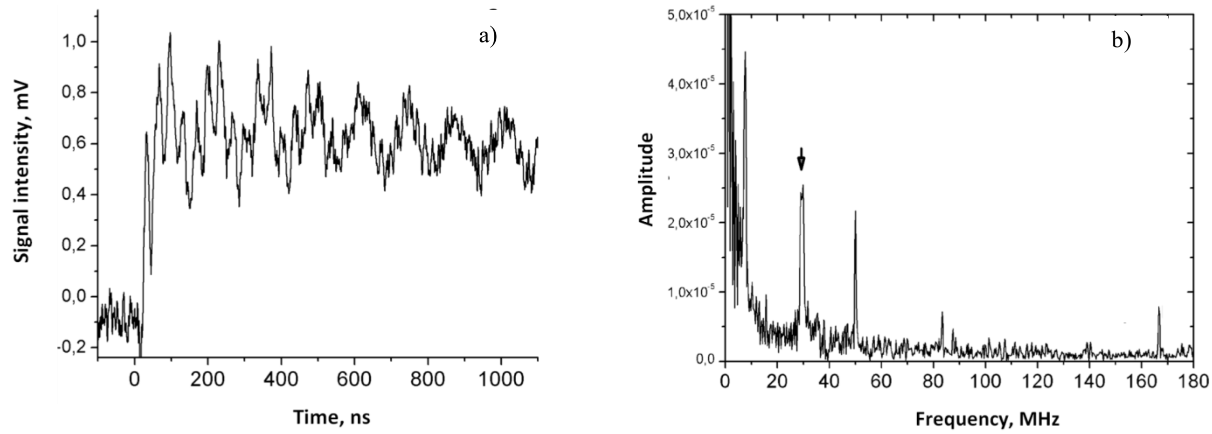

Fig. 5. a) Acoustic signal with a grating period of 50 µm, b) Fourier spectrum.

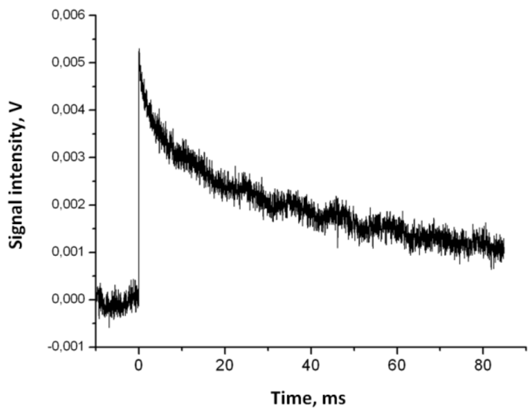

Fig. 6. Kinetics of long-lived lattice relaxation in laser-modified CdZnTe samples.

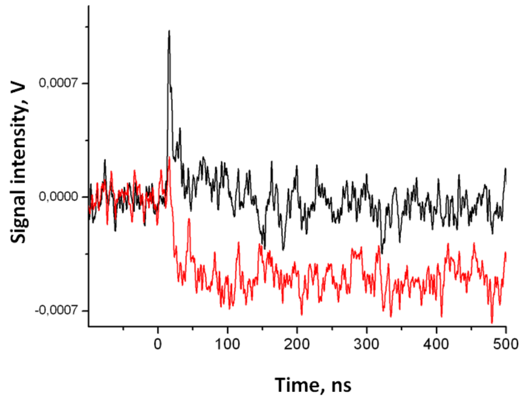

Fig. 7. Attenuation kinetics of the phase (red) and amplitude (black) gratings. The gratings are shifted relative to each other by π/2. (The zero line corresponds to the background level.)

3. Study of photoluminescence

During the laser pulse, CdTe emits radiation ("edge" luminescence), the intensity of which depends on the excitation flux density and the number of irradiation sessions. The dependence of the photoluminescence intensity on the irradiation energy density is shown in Fig. 8.

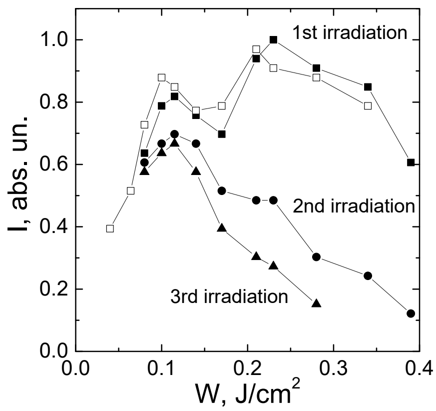

Fig. 8. Dependence of the photoluminescence intensity of cadmium telluride on the energy density of laser irradiation.

During the first irradiation session (0.08 to 0.4 J/cm^2), the photoluminescence intensity of CdTe exhibits two maxima at the energy densities of 0.1 and 0.21 J/cm^2. A repeated series of measurements carried out for another irradiation zone (with the energy densities ranging from 0.04 to 0.4 J/cm^2) confirms this finding. It should be noted that the photoluminescence intensity peaks are reached before melting. The observed minimum is possibly related to reaching certain critical temperature, at which photoluminescence is quenched (Fig. 8).

The decrease in the intensity of the first peak and the disappearance of the second one are observed upon repeated irradiation. This is apparently due to surface remelting, which results in both violation of the stoichiometric composition and emergence of various types of point defects in the semiconductor surface layer, which quench photoluminescence.

4. Conclusions

The most important results obtained in this study are as follows:

1. The features of dynamics of the reflection coefficient in laser-modified A^2B^6 semiconductors have been analyzed. The observed dynamics of the reflection coefficient is caused by its temperature dependence as well as interference phenomena in the melt–solid structure.

2. The thermal conductivity of the samples (Zn content less than 4%) was measured using the induced dynamic grating method. The obtained results are in good agreement with the known experimental data. The relaxation time of the excited thermal grating in the initial and laser-modified samples was found to be the same.

3. Using the induced dynamic grating method, it was found that a long-term electron grating with the relaxation time up to 10 ms can be formed in laser-modified samples.

References

1. Ahmed B.A., Shallal I.H., AL-Attar F.I.M. Physical properties of CdS/CdTe/CIGS thin films for solar cell application. 2018. *J. Phys.: Conf. Ser.* **1032**. P. 012022. https://doi.org/10.1088/1742-6596/1032/1/012022.
2. Gnatyuk V., Maslyanchuk O., Solovan M. *et al.* CdTe X/γ-ray detectors with different contact materials. *Sensors*. 2021. **21**. P. 3518. https://doi.org/10.3390/s21103518.
3. Alharbi T. Energy resolution improvement of CdTe detectors by using the principal component analysis technique. *Nucl. Instrum. Methods Phys. Res. A*. 2018. **882**. P. 114–116. https://doi.org/10.1016/j.nima.2017.11.027.
4. Sklyarchuk V., Gnatyuk V., Aoki T. Spectrometric properties of single and series-connected Cr/CdTe/Au Schottky-diode detectors. *Proc. SPIE: Optical Engineering + Applications*. 2024. **13151**: Hard X-Ray, Gamma-Ray, and Neutron Physics XXVI. https://doi.org/10.1117/12.3027469.

5. Sklyarchuk V., Gnatyuk V., Aoki T. Effect of the metal nature on the I-V characteristics of CdTe diodes for ionizing radiation detectors. *Proc. SPIE*. 2023. **12696**. P. 126960L-1. https://doi.org/10.1117/12.2676538.
6. Kurková D., Judas L. X-ray tube spectra measurement and correction using a CdTe detector and an analytic response matrix for photon energies up to 160 keV. *Radiat. Meas.* 2016. **85**. P. 64–72. https://doi.org/10.1016/j.radmeas.2015.12.008.
7. Sklyarchuk V., Gnatyuk V., Fochuk P.M., Aoki T. Characterization of Schottky-diode X/γ-ray detectors based on CdTe crystals with different uncompensated impurity concentrations. *Nucl. Instrum. Methods Phys. Res. A*. 2022. **1027**. P. 166229. https://doi.org/10.1016/j.nima.2021.166229.
8. Roy U.N., Camarda G.S., Cui Y. *et al*. Impact of selenium addition to the cadmium-zinc-telluride matrix for producing high energy resolution X-and gamma-ray detectors. *Sci. Rep.* 2021. **11**. P. 10338. https://doi.org/10.1038/s41598-021-89795-z.
9. Levytskyi S., Cao Z., Biriukov O. Features of the origin and propagation of a shock wave in semiconductors during nanosecond laser irradiation. *Phys. Chem. Solid State*. 2025. **26**, No 1. P. 43–48. https://doi.org/10.15330/pcss.26.1.43-48.
10. Kamel R.E.E., Ibrahim E., Eliwa A.Y. *et al.* Structural, optical and electrical properties of Cadmium Sulfide thin films synthesized by thermal evaporation technique. *Sohag J. Sci.* 2026. **11**. P. 30–36. https://doi.org/10.21608/sjsci.2026.439084.1325.
11. Furukawa K., Buitrago-Casas J.C., Vievering J. *et al*. Development of 60 µm pitch CdTe double-sided strip detectors for the FOXSI-3 sounding rocket experiment. *Nucl. Instrum. Methods Phys. Res. A*. 2019. **924**. P. 321–326. https://doi.org/10.1016/j.nima.2018.07.011.
12. Levytskyi S.M., Zhao T., Cao Z., Stronski A.V. Modeling of diffusion motion of nanoparticles in a CdTe crystal during laser-induced doping. *Phys. Chem. Solid State*. 2021. **22**, No 2. P. 301–306. https://doi.org/10.15330/pcss.22.2.301-306.
13. Veleschuk V.P., Gnatyuk V.A., Aoki T. *et al.* Melting threshold and thermal conductivity of CdTe under pulsed laser irradiation. *Lecture Notes in Networks and Systems*. 2020. **101**. P. 101–109. https://doi.org/10.1007/978-3-030-36841-8_10.
14. Levytskyi S., Cao Z., Koba A., Koba M. Dependence of the melting threshold of CdTe on the wavelength and pulse lifetime of laser radiation. *Mater. Rep.* 2024. **38**, No 7. P. 22120127 (1–6). https://doi.org/10.11896/cldb.22120127.
15. Gnatyuk V. In/CdTe/Au *p-n* junction-diode X/γ-ray detectors formed by frontside laser irradiation doping. *Nucl. Instrum. Methods Phys. Res. A*. 2022. **1029**. P. 166397. https://doi.org/10.1016/j.nima.2022.166397.
16. Levytskyi S. Thermodynamic and kinetic processes of modifying cadmium telluride based heterosystems initiated by nanosecond intense laser radiation. *SPQEO*. 2025. **28**. P.432–440. https://doi.org/10.15407/spqeo28.04.432.

Author and CV

Serhii M. Levytskyi, PhD, Senior Researcher at the Department of Optoelectronics, V. Lashkaryov Institute of Semiconductor Physics, NAS of Ukraine. Author of more 150 publications and 6 patents. Field of research: technologies of synthesis of II-VI and IV-VI semiconductors, experimental and theoretical investigation of photoelectric, electrical, optical and structural properties of these semiconductors, nanosecond laser processing, laser-induced doping of CdTe, metal-semiconductor contacts and diode structures, as well as IR and X/γ-ray detectors.
http://orcid.org/0000-0002-3909-0993

Лазерно-індуковані наносекундними імпульсами процеси масопереносу та формування інверсійних і варізонних шарів у твердих розчинах на основі телуриду кадмію

С.М. Левицький

Анотація. В даній роботі представлено результати дослідження модифікації поверхневого шару CdTe за допомогою оптичних методів, зокрема впливу лазерного опромінення на властивості CdTe з використанням методу індукованої динамічної решітки. Продемонстровано ефективність оптичного зондування у вивченні лазерно-індукованих процесів у сполуках A^2B^6. Окрім оптичних методів, для визначення властивостей досліджуваного матеріалу до та після лазерного опромінення було використано метод індукованої динамічної решітки. Також було досліджено фотолюмінесценцію лазерно-модифікованих зразків CdTe. Отримані результати суттєво розширюють сучасні уявлення про механізми взаємодії потужного лазерного випромінювання з напівпровідниковими структурами. Це відкриває перспективні можливості для прецизійного керування фізичними характеристиками матеріалів при створенні нових електронних приладів.

Ключові слова: A^2B^6, CdTe, лазерне опромінення, фотолюмінесценція, лазерне легування.